

EE

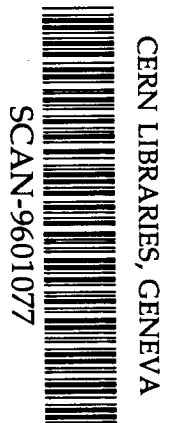


KEK Preprint 95-110  
September 1995  
H

## Neutron Beam Line at the KEK 12-GeV PS

H. NOUMI, S. SAWADA, T. HASEGAWA, N. HORIKAWA, M. IEIRI, M. ISHII,  
S. ISHIMOTO, T. IWATA, Y.D. KIM, Y. KATOH, M. KAWABATA, M.A. KOVASH,  
M. MINAKAWA, Y. MIZUNO, F. NAKAYAMA, H. OGAMI, A. OGAWA, T. SASAKI,  
T.-A. SHIBATA, Y. SUZUKI, M. TAKASAKI, K. TAMURA, K.H. TANAKA,  
J. TRICE and Y. YAMANOI

*Submitted to Nucl. Instrum. Meth., A.*



SW 9604

**National Laboratory for High Energy Physics, 1995**

KEK Reports are available from:

Technical Information & Library  
National Laboratory for High Energy Physics  
1-1 Oho, Tsukuba-shi  
Ibaraki-ken, 305  
JAPAN

Phone: 0298-64-5136  
Telex: 3652-534 (Domestic)  
(0)3652-534 (International)  
Fax: 0298-64-4604  
Cable: KEK OHO  
E-mail: [Library@kekvax.kek.jp](mailto:Library@kekvax.kek.jp) (Internet Address)

## Neutron Beam Line at the KEK 12-GeV PS

H. Noumi<sup>(1)</sup>, S. Sawada<sup>(2)</sup>, T. Hasegawa<sup>(3)</sup>, N. Horikawa<sup>(4)</sup>, M. Ieiri<sup>(1)</sup>, M. Ishii<sup>(1)</sup>,  
S. Ishimoto<sup>(1)</sup>, T. Iwata<sup>(4)</sup>, Y. D. Kim<sup>(1)\*</sup>, Y. Katoh<sup>(1)</sup>, M. Kawabata<sup>(5)</sup>, M. A. Kovash<sup>(6)</sup>,  
M. Minakawa<sup>(1)</sup>, Y. Mizuno<sup>(5)</sup>, F. Nakayama<sup>(4)</sup>, H. Ogami<sup>(7)</sup>, A. Ogawa<sup>(4)</sup>, T. Sasaki<sup>(4)†</sup>,  
T. -A. Shibata<sup>(6,7)</sup>, Y. Suzuki<sup>(1)</sup>, M. Takasaki<sup>(1)</sup>, K. Tamura<sup>(5)</sup>, K. H. Tanaka<sup>(1)</sup>,  
J. Trice<sup>(6)</sup>, and Y. Yamanoj<sup>(1)</sup>

<sup>(1)</sup>*KEK, 1-1, Oho, Tsukuba, Ibaraki 305, JAPAN*

<sup>(2)</sup>*Kyoto University, Kita shirakawa oiwake-cho, Sakyo, Kyoto 606, JAPAN*

<sup>(3)</sup>*Miyazaki University, 1-1, Gakuen kinohanadai nishi, Miyazaki 889-21, JAPAN*

<sup>(4)</sup>*Nagoya University, Furo-cho, Chigusa, Nagoya 464-01, JAPAN*

<sup>(5)</sup>*RCNP, Osaka University, 10-1, Mihogaoka, Ibaraki, Osaka 567, JAPAN*

<sup>(6)</sup>*University of Kentucky, Lexington, KY 40506, U.S.A.*

<sup>(7)</sup>*Tokyo Institute of Technology, 2-12-1, Ookayama, Meguro, Tokyo 152, JAPAN*

### Abstract

A neutron beam line has been constructed at the KEK-Proton Synchrotron. Neutrons have been produced by the disintegration reactions of deuterons in a 6 cm thick beryllium target. Deuteron beams of 2 ~ 6 GeV have provided neutron beams of 1 ~ 3 GeV. The neutron flux increases with the deuteron energy. The typical beam intensities obtained were  $1 \times 10^8$ ,  $2 \times 10^8$ , and  $3 \times 10^8$  neutrons per  $10^{11}$  deuterons of 2, 4, and 6 GeV, respectively. The neutron-momentum width,  $\Delta p/p$ , was measured to be  $(4 \pm 1)\%$  in sigma at 1 GeV.

---

\*present address: *Seoul National University, Seoul 151-742, KOREA*

†present address: *Toyota Central Research & Development Labs., Inc., Nagakute-cho, Aichi 480-11, JAPAN*

## 1 Introduction

The deuteron beam has been successfully accelerated since the end of 1991 at the KEK 12-GeV proton synchrotron (KEK-PS) [1]. This success opened a new possibility to accelerate light-to-heavy ions and to utilize the ion-beams for various experimental programs at the KEK-PS.

For a utilization of the deuteron beam, a neutron beam line has been constructed at the KEK-PS P1 beam line [2]. The beam line was designed for an experiment to measure the differential cross sections of deuteron productions via  $(n, \gamma)$  reactions on liquid hydrogen (E235 [3]), which was carried out in April, 1993. Neutrons were produced via the disintegration reaction of deuterons in a beryllium target. A neutron beam line has existed at the Saclay/Saturne [4], which provides monokinetic neutrons produced via the same reaction in which the deuteron-energy region covers up to  $\sim 2$  GeV. Since deuteron beams of  $2 \sim 11.2$  GeV can be supplied by the KEK PS, neutrons of  $1 \sim 5.6$  GeV are available at the P1 beam line. Beside the E235 experiment, the neutron beam can be used for various purposes: the interactions of a neutron with a nucleus have so far been estimated only approximately using those of a proton since no data are available in the several-GeV region with neutrons. Systematic studies of neutron-nucleus interactions have to be made. Furthermore, monokinetic neutrons would be quite useful for other field such as nuclear engineering as well as for physics.

In this paper we report the features of the constructed beam line and the characteristics of the deuteron and neutron beams obtained in beam-line tunings for the E235 experiment, in which 2.0, 4.0, 4.7, 5.4 and 6.0-GeV deuterons were used.

## 2 Design Principle

We used the proton-stripping reaction of deuterons in a beryllium target to produce the neutron beam in the several-GeV region. Spectator neutrons in the proton-stripping reaction of deuterons reflect the Fermi motion in the deuteron; the momentum and angular spreads of the neutrons are mainly caused by the Fermi motion. The momentum and angular spreads become relatively small when the beam momentum is much higher than the Fermi momentum. The relativistic deuteron beams provided by the KEK-PS were therefore suited for the present purpose.

We performed a Monte-Carlo simulation in order to understand the neutron beam obtained in the proton-stripping reaction of deuterons in a beryllium target. The simulation included the effects of: (i) the Fermi motion of a neutron in a deuteron, (ii) the fluctuation of the deuteron-energy loss and multiple scattering in a beryllium target, and (iii)

the energy spread of the deuteron beam ( $\sigma \sim 0.3\%$ ). A neutron collimator was designed by using the simulation [5]. The collimator defined the momentum distribution as well as the spatial distribution of the neutron beam. The structure of the neutron collimator is described in the next section. In order to obtain the neutron-momentum distribution in a deuteron, Hulthén's wave function [6] was employed, which is written as

$$\psi(r) = \sqrt{\frac{\alpha}{\pi}} \frac{e^{-\alpha r}}{r}, \quad (1)$$

where  $r$  represents the relative distance between the two nucleons, and  $\alpha^{-1} = 4.3$  fm ( $\alpha\hbar = 46$  MeV/c) was used. From the Fourier transformation of  $\psi$ , the neutron-momentum distribution in the deuteron-rest frame can be written as

$$f(p)dp^* = C \frac{p^{*2}}{[p^{*2} + (\alpha\hbar)^2]^2} dp^*. \quad (2)$$

Here,  $C$  represents a normalization factor. Interactions of neutrons with the target, the collimator, and other relevant materials were simulated by using the GEANT computer code [7]. Fig. 1 shows neutron-beam momentum distributions at the experimental target, simulated for 2, 4, and 6-GeV deuteron beams. The solid lines fit the simulated spectra very well. For the fitting a following function was used:

$$F(p)dp = C \frac{\gamma_d^3 p^2}{[(p - p_c)^2 + (\gamma_d \alpha \hbar)^2]^2} dp, \quad (3)$$

where  $\gamma_d = (1 - \beta_d)^{-1/2}$ ,  $\beta_d$  being the deuteron's velocity, and  $p_c$  is the central value of the neutron-beam momentum distribution. The function  $F(p)$  corresponds to the Lorentz transformation of the longitudinal component of  $f(p^*)$ , in which  $p^* = (p - p_c)/\gamma_d$ . The neutron collimator realized this condition since only neutrons produced at around 0 degrees could path through the collimator.

### 3 Beam Line

Fig. 2 illustrates the P1 beam line with the neutron beam line. The deuteron beam extracted from the KEK-PS was transported to the P1 beam line, and then focused onto a neutron production (Be) target. The beam-spot size on the beryllium target was controlled with three quadrupole magnets (Q1~3). The deuteron-beam intensity was controlled with the CH and CV collimators placed after the Q3 magnet. The S1 and D1 steering magnets were used to adjust the beam position at the target in the vertical and horizontal directions, respectively. The CH collimator was installed in the gap of the S1 magnet so as to save beam-line space. It was driven by a motor in a vacuum duct of the beam line.

The deuteron-beam intensity was measured by secondary emission chambers (SEC) [8]. SEC was calibrated by the foil-activation method with approximately 10% accuracy. The errors came mostly from the referred cross sections of the  $^{24}\text{Na}$ -production reaction by deuterons on  $^{27}\text{Al}$  [9]. Details concerning the calibration have been reported elsewhere [10, 11]. A deuteron-beam profile was monitored using segmented parallel plate ionization chambers (SPIC) [12]. A beryllium target of 3 cm diameter and 6 cm length was used. A target monitor (TM) was placed at 90 degrees to the beam line in order to confirm that the beam hit the correct position. TM was a counter telescope consisting of three small plastic scintillators. The neutron yield was maximized at the highest counting rate of TM, as indicated in Fig. 3. The neutron-beam monitor (NBM) shown in the figure is described in the next section.

The deuteron beam was focused onto the beryllium target by using the Q1~Q3 magnets. It was advantageous for the E235 experiment to have a rather parallel deuteron beam on the beryllium target even though the beam spot size was large, since the neutron production probability in the proton-stripping reaction is maximum at 0 degrees. A deuteron-beam envelope for the E235 experiment calculated by using the TRANSPORT computer code[13] was illustrated in Fig. 4. The beam was tuned so as to realize an image size of about 20 mm in diameter at the beryllium target. It was nearly as large as the target diameter. A deuteron-beam profile at the target was measured by SPIC, as shown in Fig. 5.

Charged particles from the beryllium target were swept out in the vertical direction by the D2 bending magnet located just downstream of the target, and only neutrons produced at around 0 degrees could pass through the collimator with a length of 5 m (Fig. 6). It comprised cast lead surrounded by iron. The loophole of the collimator was gradually widened along the beam line, which was 34(Horizontal) $\times$ 34(Vertical) mm<sup>2</sup> at the entrance and 52(H) $\times$ 52(V) mm<sup>2</sup> at the exit. The solid angle for the neutrons was approximately 50  $\mu\text{sr}$ . Although the D3 magnet was placed as a secondary sweeping magnet, it was not used because the neutron beam was already sufficiently purified at this position.

An experimental target (liquid hydrogen) was located 9.85 m downstream of the neutron-production target. At an early stage of the E235 experiment NBM was placed around the hydrogen target in order to monitor the neutron-beam profiles. The spectrometer system for the experiment was installed in the P1 cave. In particular, the magnetic spectrometer placed after the hydrogen target was used to analyze the trajectories of recoiling charged particles from the target in order to investigate the neutron-beam characteristics, as described in the next section.

## 4 Neutron Beam

### 4.1 Neutron-beam profile

A set of plastic scintillator hodoscopes was employed as a neutron-beam monitor (NBM) [14]. NBM comprised 3 layers in the beam direction. The first, second, and third layers respectively had cross sections of  $210(\text{H})\times 380(\text{V})\text{ mm}^2$ ,  $200(\text{H})\times 200(\text{V})\text{ mm}^2$ , and  $204(\text{H})\times 260(\text{V})\text{ mm}^2$ . The second layer had a thickness of 10 mm, and the others had 2 mm. The first layer was used as a veto counter for charged particles that remained in the neutron beam. It was divided into 16 slabs in the horizontal direction. The second layer was divided into 13 slabs in the vertical direction. This layer acted as a converter of neutrons to charged particles by their interactions with hydrogen and carbon nuclei in the scintillator, and gave a neutron detection efficiency of about 1%. The last layer was divided into two halves vertically and also into 13 slabs horizontally. This layer was sensitive to the charged particles from the reaction in the second layer. NBM provided a neutron-beam profile, as shown in Fig. 7.

A neutron-beam profile can be also obtained from the reaction vertex in the  $(n, X)$  reactions on the hydrogen (H) target. Figure 8 shows the two-dimensional distribution of the reaction vertex obtained from the track reconstruction. The precision of the vertex position in the vertical and horizontal directions is about 1 cm. The hydrogen target vessel is a vertical cylinder of 12 cm diameter. It is confirmed that the neutron beam is well collimated and is not hitting the wall of the hydrogen-target vessel because no enhancement of the vertex distribution on the wall is seen.

Both the measured profiles were consistent with the image of the neutron collimator.

### 4.2 Neutron-beam intensity

NBM was also used as a neutron-intensity monitor. The ratio of the neutron intensity to the deuteron-beam intensity can be obtained using

$$\frac{I_n}{I_d} = N_{\text{Be}} \left. \frac{d\sigma}{d\Omega} \right|_{\theta=0^\circ} \Delta\Omega, \quad (4)$$

where  $N_{\text{Be}}$  is the number of beryllium nuclei in the target, and  $d\sigma/d\Omega|_{\theta=0^\circ}$  represents the differential cross section of the neutron-production reaction,  $d + \text{Be} \rightarrow n + X$ , at 0 degrees. The quantity  $\Delta\Omega$  stands for the solid angle of the neutron collimator. Differential cross sections have been reported for neutron momenta of 1.35 GeV/c [15], 1.77 GeV/c [16], and 2.90 GeV/c [17]. Parametrizing the cross section,  $I_n/I_d$  was calculated as a function of the deuteron energy, as listed in Table 1. The efficiency of NBM for neutron detection was calibrated in this way. It was found to be about 1% in the present energy region. Details

concerning an evaluation of the efficiency are described in ref. [14]. Once the efficiency is known, NBM can be used as an intensity monitor. The neutron intensity increased with the deuteron energy. Typical beam intensities were obtained to be  $1 \times 10^8$ ,  $2 \times 10^8$ , and  $3 \times 10^8$  neutrons per  $10^{11}$  deuterons of 2, 4, and 6 GeV, respectively. The errors in the measured intensities came mainly from the errors of the neutron-production cross sections used and the errors in the deuteron intensity measured by SEC. The errors were about 30% in total. The measured intensities agreed with the expected values within the errors.

NBM was also used to measure the contamination of charged particles in the neutron beam. In this case, the first scintillator hodoscope was used as a charged-particle counter in coincidence with the other hodoscopes. The contamination of charged particle was found to be less than 1% and about 2% for 1 and 3-GeV neutron beams, respectively.

### 4.3 Momentum distribution of the neutron beam

The momentum distributions of the neutron beams were measured by analyzing the momenta of recoiling protons in  $(n, p)$  elastic reactions on hydrogen. Fig. 9 shows a measured spectrum of the missing mass in the final state in the  $(n, p)$  reactions on hydrogen at 1 GeV. Background events which occurred on the materials other than the liquid-hydrogen target were evaluated and corrected by using target-empty data. A peak of the neutron in the final state of the  $(n, p)$  elastic scattering can be seen at  $0.94 \text{ GeV}/c^2$  in the spectrum. The neutron-beam momentum width was obtained to be  $(5.8 \pm 1)\%$  in sigma from the neutron-peak width in the missing-mass spectrum, assuming a Gaussian function for the peak. The error was the fitting error due mainly to a broad  $N^*$  peak lying above the neutron peak. The width includes the effect of the finite momentum resolution of the magnetic spectrometer. The momentum resolution of the spectrometer was evaluated to be  $(4 \pm 1)\%$  by a Monte-Carlo simulation which included the spatial resolution of the drift chambers and systematic errors such as inaccuracy of the chamber alignment. After the spectrometer resolution was subtracted, we obtained  $(4 \pm 1)\%$  in sigma ( $(10 \pm 3)\%$  in FWHM) as the neutron-beam momentum width at 1 GeV. At higher energy, the width is expected to be smaller when expressed in percentage, since the Fermi motion of the neutron in the deuteron remains the same. The Model calculation with the deuteron wave function mentioned in section 2 indicated a neutron-beam width of 7.2% (FWHM) at 1 GeV. (The calculation gave an r.m.s. width of 5.4%, which was larger than the measured width, since the simulated spectrum has a longer tail than the Gaussian distribution.) The measured width does not contradict the calculated value.



## 5 Summary

We constructed a neutron beam line at the KEK-PS P1 beam line. Neutron beams of 1~3 GeV were delivered to the P1 Cave. The flux was typically  $1 \times 10^8$ ,  $2 \times 10^8$ , and  $3 \times 10^8$  neutrons per  $10^{11}$  deuterons of 2, 4, and 6 GeV, respectively. The neutron-beam momentum width,  $\Delta p/p$ , was measured to be  $(4 \pm 1)\%$  in sigma. The measured value agrees with the Model calculation with the deuteron wave function.

The neutron beam line provides neutron beams with good intensity and a small momentum spread at the several-GeV region. Thus, it provides unique experimental opportunities to investigate neutron-nucleon and/or neutron-nucleus interactions. Furthermore, one can expect a polarized neutron beam if a polarized deuteron beam is accelerated in the KEK-PS [18]. The polarized beam would provide a possibility to measure the spin observables and symmetries on nucleon-nucleon, nucleon-nucleus, and quark-quark interactions.

## Acknowledgements

The authors thank Professors H. Sugawara, Professor S. Iwata, Professor K. Nakai and the crew of the KEK-PS experimental group for their support for this project. They are also grateful to Professor M. Kihara and the members of the KEK-PS accelerator group for their efforts for the successful acceleration of the deuteron beam. They thank Professor K. Kondo and the crew of the KEK radiation safety control center for their work concerning the modification of the P1 beam line and the SEC calibration by the foil-activation method.

## References

- [1] Y. Mori, "Acceleration of deuteron beam in the KEK proton synchrotron", KEK Preprint 91-159.
- [2] M. Takasaki *et al.*, KEK Internal Report 92-5 (in Japanese); F. Abe *et al.*, Nucl. Instr. and Meth. 220 (1984) 293.
- [3] M. A. Kovash (spokesperson) *et al.*, KEK-PS Proposal E235, (1990).
- [4] G. Bizard *et al.*, Nucl. Instr. and Meth. III (1973) 451.
- [5] Y. Mizuno, "Unpolarized Neutron Beam Line and Simulation in the Region of  $E_n = 1 \sim 5$  GeV at KEK-PS". 1992, unpublished.

- [6] L. Hulthén and M. Sugawara, "The Two-Nucleon Problem", Encyclopedia of Physics, Vol.XXXIX, p.1, edited by S. Flügge, Springer-Verlag, 1957.
- [7] R. Brun *et al.*, GEANT3 User's Guide, CERN DD/EE/84-1.
- [8] V. Agoritsas and R. L. Witkover, IEEE Trans. Nucl. Sci. NS-26 (1979) 3355. H. Hirabayashi *et al.*, Jour. Phys. Soc. of Japan, 51 (1982) 3098 and refs. therein.
- [9] P. Kozma and J. Kliman, J. Phys. G:Nucl. Part. Phys., 16 (1990) 45; J. Banaigs *et al.*, Nucl. Instr. and Meth. 95 (1971) 307.
- [10] M. Numajiri *et al.*, Proceedings of the 9th Symposium on Accelerator Science and Technology, KEK, August, 1993, p.428, and references therein.
- [11] M. Ieiri *et al.*, Proceedings of the 9th Symposium on Accelerator Science and Technology, KEK, August, 1993, p.477, and references therein.
- [12] K. H. Tanaka *et al.*, Proceedings of the Workshop on Advanced Beam Instrumentation, KEK, April, 1991, edited by A. Ogata and J. Kishiro, p.145.; K. H. Tanaka *et al.*, "Improvement in the Profile and Emittance Measurement System of the KEK-PS External Beam Line", KEK Preprint 91-27
- [13] K. L. Brown, F. Rothacker, D. C. Carey and Ch. Iselin, TRANSPORT, CERN 80-04.
- [14] T. Sasaki *et al.*, "A profile and flux monitor of the neutron beam in a few GeV region at KEK", KEK Preprint 94-188; T. Sasaki *et al.*, Nucl. Instr. and Meth. A in press.
- [15] G. Bizard *et al.*, Nucl. Instr. and Meth. III (1973) 445.
- [16] R. L. Lander *et al.*, Phys. Rev. 137B 1228(1965).
- [17] Bevalac Users manual, p.H 8.
- [18] H. Sato *et al.*, KEK-PS Proposal T323, (1991).

## Table Captions

Table 1 Expected neutron intensity relative to the deuteron-beam intensity as a function of the deuteron energy. The values were used to calibrate the efficiency of the neutron-beam monitor (NBM).

$P_n$ (GeV/c)	$E_d$ (GeV)	$I_n/I_d$
1.70	2.0	$(1.16 \pm 0.31) \times 10^{-3}$
2.79	4.0	$(2.14 \pm 0.58) \times 10^{-3}$
3.15	4.7	$(2.46 \pm 0.67) \times 10^{-3}$
3.52	5.4	$(2.79 \pm 0.75) \times 10^{-3}$
3.83	6.0	$(3.07 \pm 0.84) \times 10^{-3}$

Table 1

## Figure Captions

- Fig. 1 Neutron-momentum spectra (histogram) obtained by Monte-Carlo simulations for proton-stripping reactions of deuterons in the beryllium target. The quoted energies, 2, 4, and 6 GeV, indicate the deuteron-beam energy used in the simulation. Solid lines fit the spectra with a function characterized by eq. 3.
- Fig. 2 P1 beam line with the neutron beam line newly constructed at the KEK-PS. The deuteron beam from the KEK-PS was transported to the P1 beam line, and then focused with the Q1~Q3 quadrupole magnets onto a beryllium (Be) target of 3 cm diameter and 6 cm length. The deuteron beam was monitored by SEC, SPIC, and TM (see text in detail for these monitors). The CH and CV collimators controlled the deuteron-beam intensity. The S1 and D1 steering magnets were used to adjust the deuteron-beam position. The D2 and D3 magnets swept out charged particles from the beryllium target. Only neutrons produced at around 0 degrees could pass through the lead (Pb) collimator which is 5 m long. The spectrometer system for the E235 experiment was installed in the P1 Cave. A liquid hydrogen target was installed 9.85 m downstream of the beryllium target. The magnetic spectrometer (indicated as "D spectrometer") was placed after the hydrogen target in order to analyze charged particle trajectories from the hydrogen target.
- Fig. 3 Neutron yield measured by NBM is compared to the counting rate of TM as a function of the target position. The target was scanned vertically with respect to the beam axis.
- Fig. 4 Deuteron-beam envelope for the E235 experiment calculated with TRANSPORT.
- Fig. 5 Deuteron-beam profile measured by SPIC at the beryllium target.
- Fig. 6 Schematic view of the cross section of the neutron collimator along the beam line.
- Fig. 7 Neutron-beam profiles obtained by a set of plastic scintillator hodoscopes (NBM).
- Fig. 8 Two-dimensional distribution of the reaction vertex of the  $(n, X)$  reaction on the hydrogen target.
- Fig. 9 Missing mass spectrum measured in the elastic  $(n, p)$  reaction on hydrogen at the neutron-beam energy of 1 GeV. A peak which corresponds to the neutron in the final state is seen at  $0.94 \text{ GeV}/c^2$ .

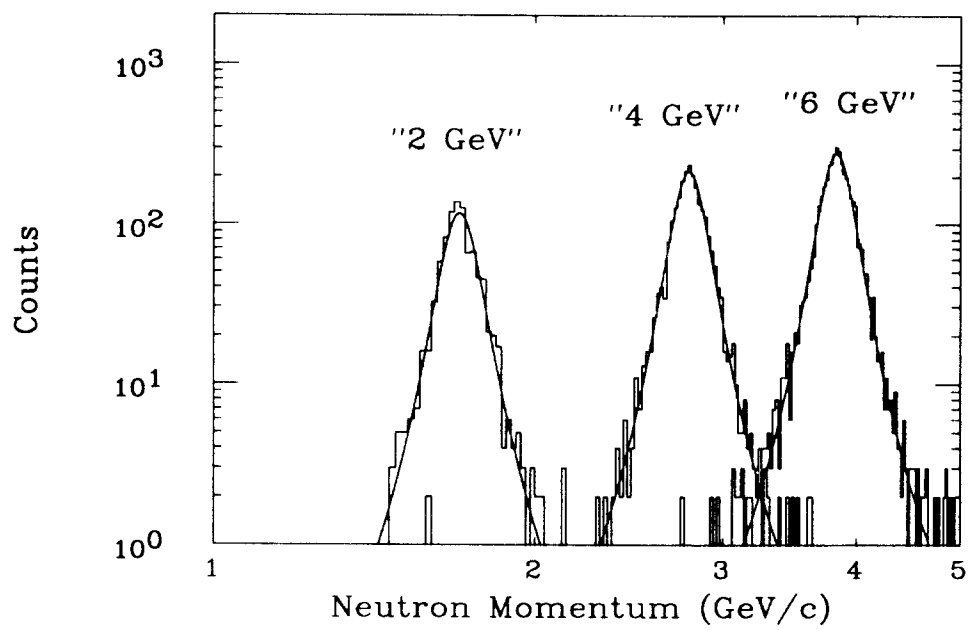


Figure 1:

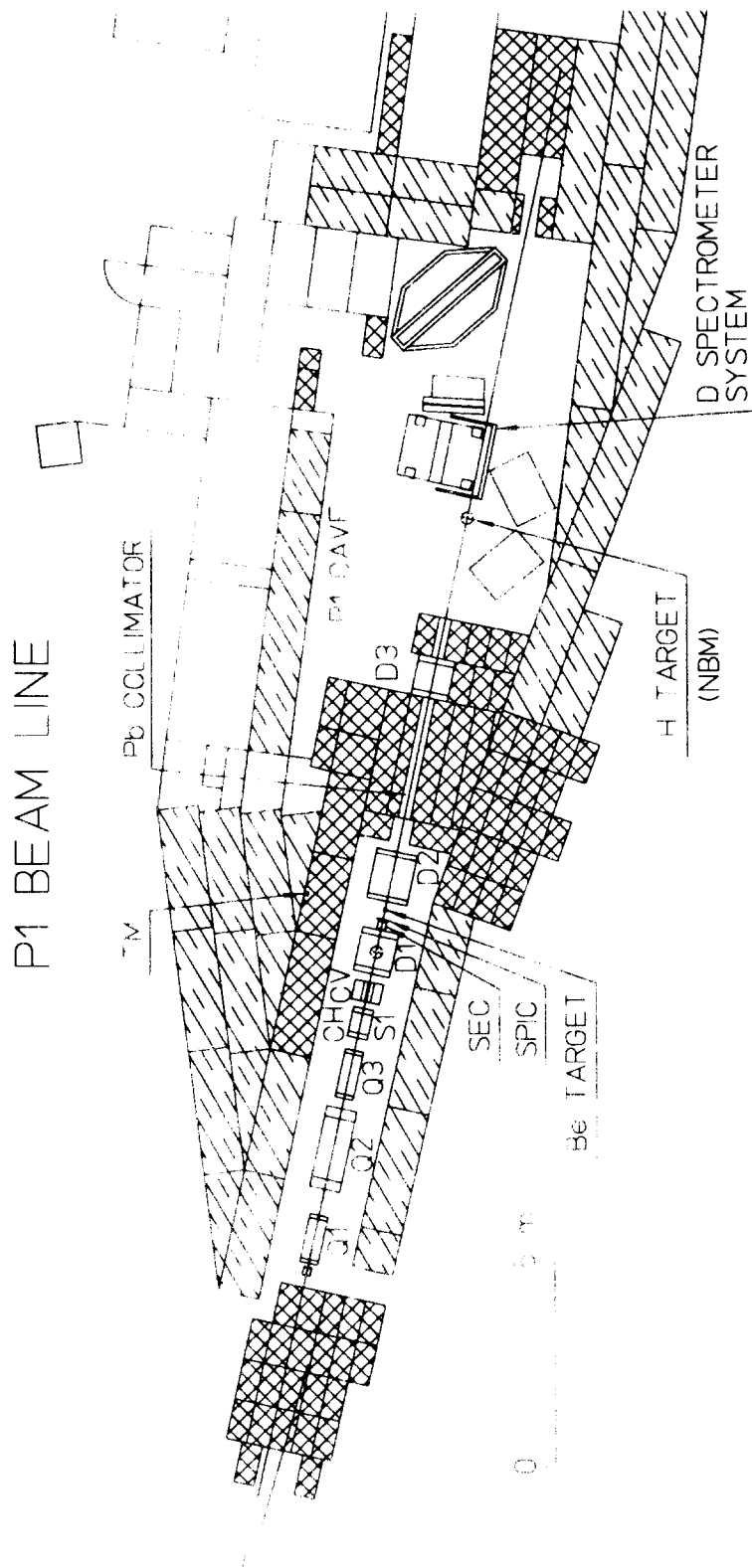


Figure 11

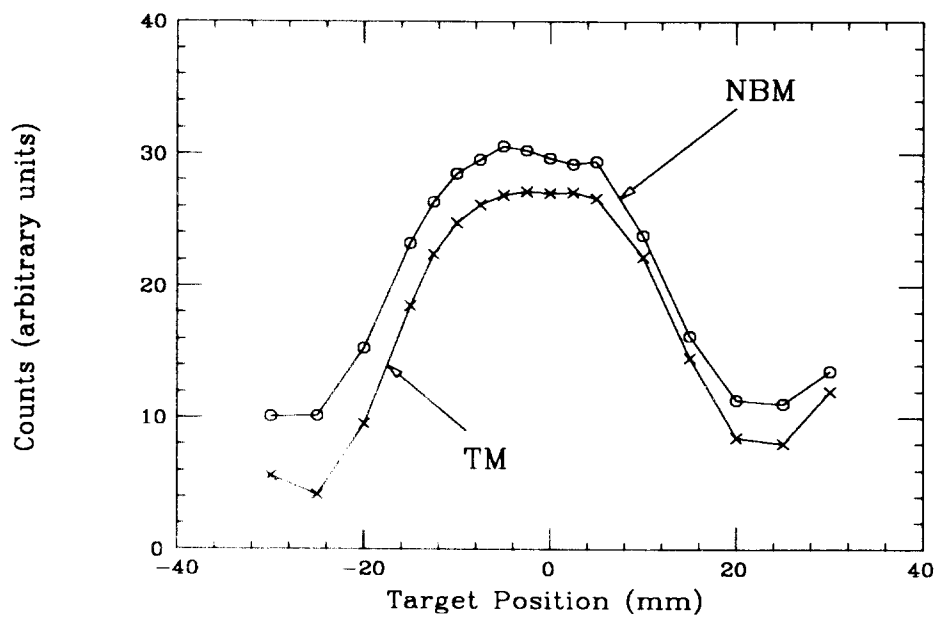


Figure 3

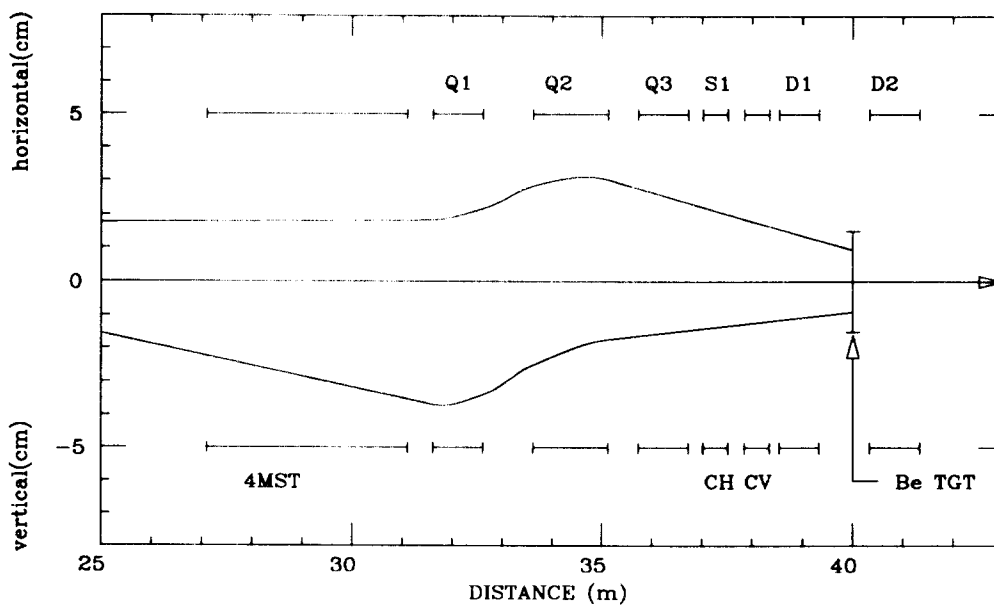


Figure 4

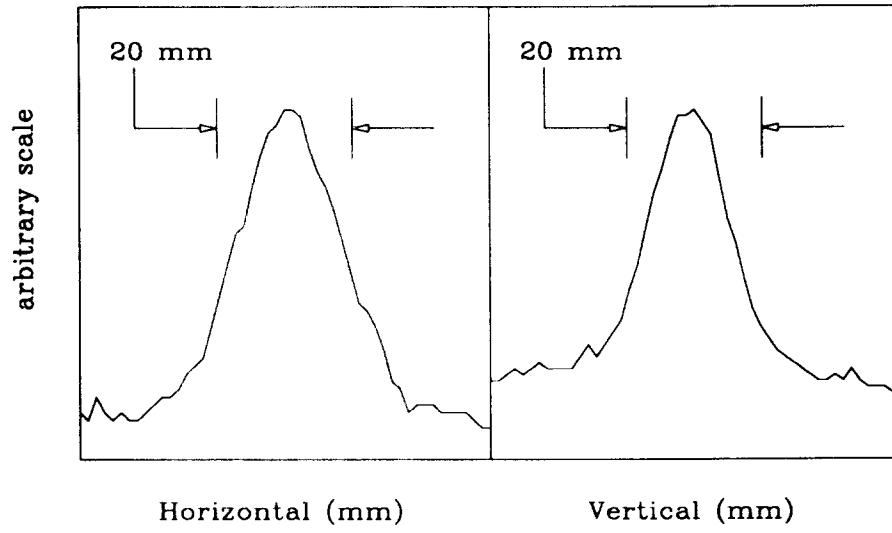


Figure 5

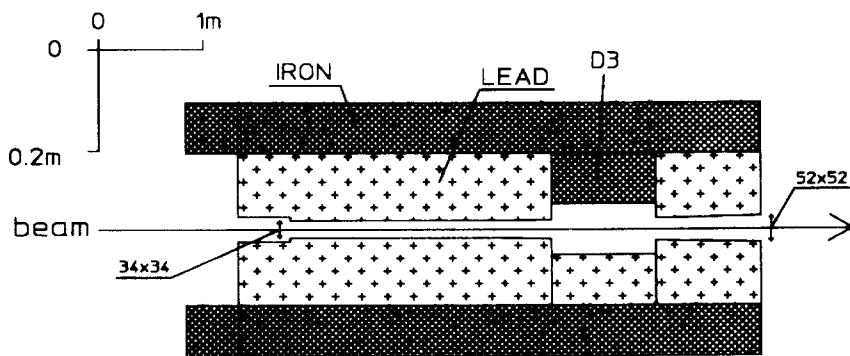


Figure 6:



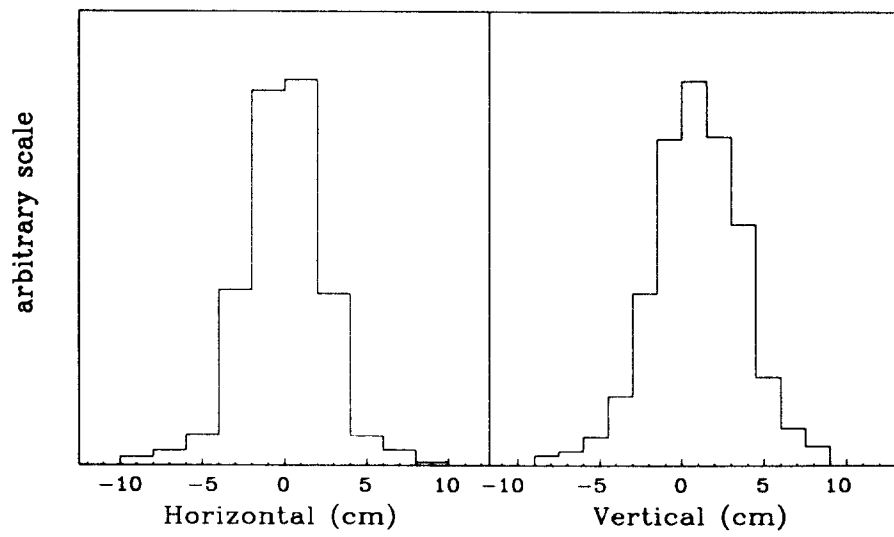


Figure 7.

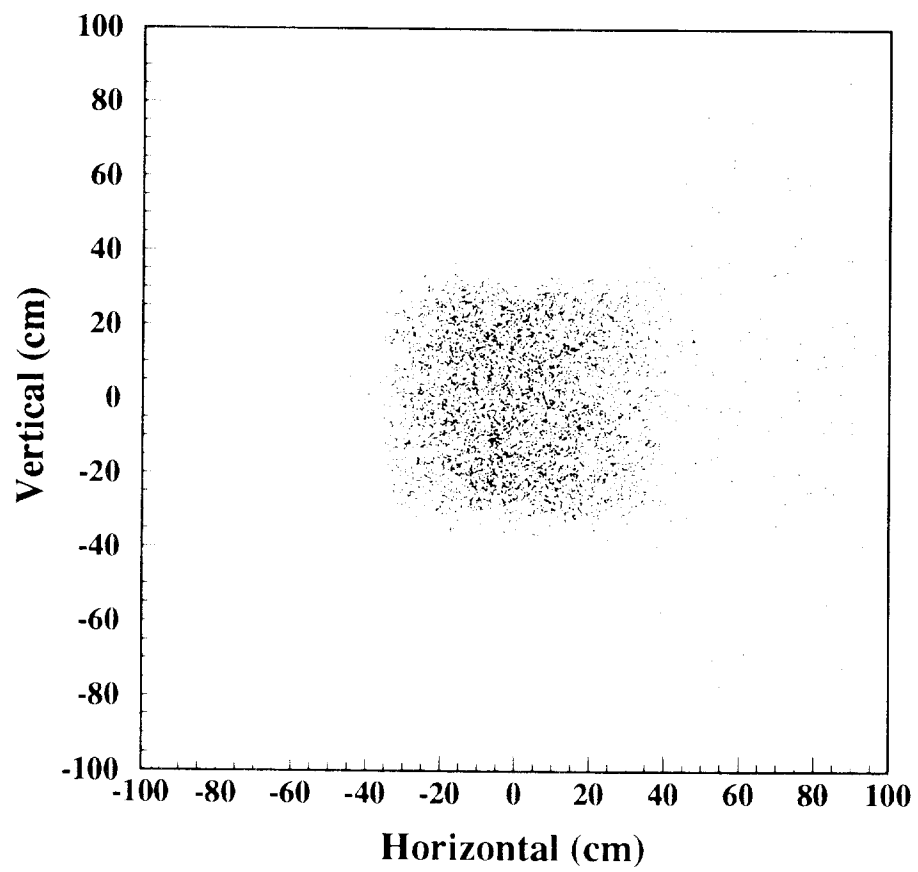


Figure 8:

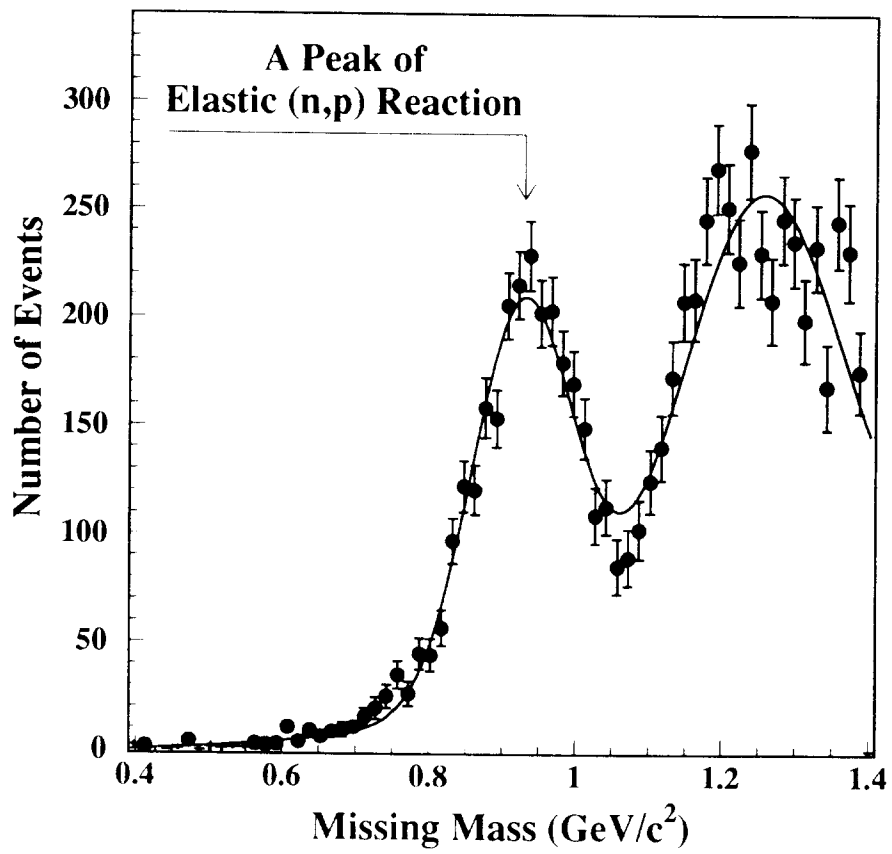


Figure 9

